# Performance Analysis of Recurrence Matrix Statistics for the Detection of Deterministic Signals in Noise

JOSEPH V. MICHALOWICZ

*SFA, Inc.*
*Crofton, Maryland*

JONATHAN M. NICHOLS

*Optical Techniques Branch*
*Optical Sciences Division*

FRANK BUCHOLTZ

*Photonics Technology Branch*
*Optical Sciences Division*

January 4, 2008

# REPORT DOCUMENTATION PAGE

| 1. REPORT DATE (DD-MM-YYYY) 04-01-2008 | 2. REPORT TYPE Memorandum Report | 3. DATES COVERED (From - To) 1 January 2007 – 15 August 2007 |
|---|---|---|

**4. TITLE AND SUBTITLE**

Performance Analysis of Recurrence Matrix Statistics for the Detection of Deterministic Signals in Noise

**5a. CONTRACT NUMBER**

**5b. GRANT NUMBER**

**5c. PROGRAM ELEMENT NUMBER**
ONR 61135N

**6. AUTHOR(S)**

Joseph V. Michalowicz,* Jonathan M. Nichols, and Frank Bucholtz

**5d. PROJECT NUMBER**

**5e. TASK NUMBER**

**5f. WORK UNIT NUMBER**
WU EW014-02-41-8955

**7. PERFORMING ORGANIZATION NAME(S) AND ADDRESS(ES)**

Naval Research Laboratory
4555 Overlook Avenue, SW
Washington, DC 20375-5320

SFA, Inc.
2200 Defense Highway
Crofton, MD 21114

**8. PERFORMING ORGANIZATION REPORT NUMBER**

NRL/MR/5650--08-9098

**9. SPONSORING / MONITORING AGENCY NAME(S) AND ADDRESS(ES)**

Office of Naval Research
One Liberty Center
875 North Randolph Street
Arlington, VA 22203-1995

**10. SPONSOR / MONITOR'S ACRONYM(S)**
ONR

**11. SPONSOR / MONITOR'S REPORT NUMBER(S)**

**12. DISTRIBUTION / AVAILABILITY STATEMENT**

Approved for public release; distribution is unlimited.

**13. SUPPLEMENTARY NOTES**

*SFA, Inc., 2200 Defense Highway, Crofton, MD 21114

**14. ABSTRACT**

Understanding the limitations to detecting deterministic signals in the presence of noise, especially additive, white Gaussian noise, is of importance for the design of LPI systems and anti-LPI signal defense. In this report, we investigate the use of recurrence plots for such detection, and we compare the performance of a recurrence-plot-based detector to a standard power-detection approach. Performance is evaluated using receiver-operator characteristic (ROC) curves.

**15. SUBJECT TERMS**

Signal detection
Statistics

Recurrence
Receiver-operator characteristic (ROC) curves

| 16. SECURITY CLASSIFICATION OF: | | | 17. LIMITATION OF ABSTRACT | 18. NUMBER OF PAGES | 19a. NAME OF RESPONSIBLE PERSON Frank Bucholtz |
|---|---|---|---|---|---|
| **a. REPORT** Unclassified | **b. ABSTRACT** Unclassified | **c. THIS PAGE** Unclassified | UL | 30 | **19b. TELEPHONE NUMBER** (include area code) (202) 767-9342 |

**Table of Contents**

# Executive Summary

In order to avoid detection by hostile radar systems, it is essential for modern military platforms to have the capability to detect deterministic signals buried in white noise. A wide variety of detection techniques have been developed in answer to this problem; their efficiency depends on the degree of knowledge of the incoming signal. This report is applicable to the case where nothing is known *a priori* about the parameters of the incoming signal, and where the background noise is Gaussian.

Two approaches are compared. The first is a "normality" detector, which constructs a histogram of the incoming signal data points, and then compares this to the assumed Gaussian distribution of the background noise by means of a chi-squared test to determine the presence or absence of deterministic signal. The second is called the recurrence plot detector since it employs the time-delay vectors used to construct the recurrence matrix – a concept that has shown great utility for analyzing dynamical systems. This detector constructs a histogram from the distances between the time-delay vectors, and then uses a chi-squared test to compare it to the Gamma-like distribution that results when only Gaussian noise is present. The recurrence plot detector has the advantages of a larger number of data points as well as the explicit incorporation of time information in the incoming signal. Unfortunately, there may exist redundancies among the larger number of recurrence values that weaken the performance of this approach. However, by judicious choice of the embedding parameters, the deleterious effect of redundancies are shown to be minimized.

Comparison of the performance of both detectors are given for two types of incoming signals in the form of Receiver Operating Characteristic (ROC) curves. In each case, there exists a range of signal-to-noise ratios for which the recurrence plot detector offers superior performance over the normality detector, thereby demonstrating that the recurrence matrix concept has utility for signal detection. Appendices provide derivations of the relevant probability density functions as well as a procedure for constructing "ideal" Gaussian background data sets.

---

# Introduction

Detection of deterministic signals buried in white noise is an essential tactical requirement for present-day military platforms in order to avoid detection by hostile radar systems. However, current low-probability of intercept (LPI) radar systems spread the energy they transmit over a large spectral range, reducing the power in the signal to a level below the thermal noise in the target platform's radar-warning receiver.

A wide array of detection techniques exist for finding a signal in background noise. In each the general approach is the same: compute a test statistic from the data and compare it to a detection threshold. Which statistic to compute and where to set the threshold depend on the amount of *a priori* knowledge one has about the signal and on the costs assigned to a missed detection. For example, when detecting known signals in additive Gaussian noise an optimum receiver (test statistic) has been developed based on the likelihood ratio, yielding the Matched Filter. The detection threshold can be set using any one of a number of criteria for optimality including: maximum *a posteriori* (MAP), Bayes' criterion, and Neyman-Pearson criterion to name a few. An extensive literature has also evolved to handle cases where the parameters of the signal are only partially known. A thorough review is given in McDonough and Whalen[1]. The case of interest in this paper is that in which nothing is known *a priori* about the parameters of the incoming signal. This is the most difficult detection scenario, and some form of normality detector is really the only option.

This paper explores the utility of recurrence plots for detecting signals hidden in noise, when the signal is completely unknown and the background noise is Gaussian. The recurrence plot was originally constructed as a graphical tool to check stationarity in dynamical systems[2]. It essentially quantifies correlations in a time series by keeping track of when the signal "recurs"; that is, returns to a previous state. It has proven to be very useful in both depicting and analyzing complex, nonlinear, especially chaotic, systems. Examples may be found in fields as diverse as economy and earth science, astrophysics and physiology[3]. Applications of recurrence plot techniques to signal detection have also appeared in the literature[4,5,6]. Zbilut et al. used a detector based on recurrence plots to distinguish deterministic signals from noise. A detector based on cross-recurrence plots was used to extract signals from noise and was compared to a spectral detection scheme[5]. Recurrence plots were also used to distinguish signal from noise in physiologically generated signals (EMG signal) in Filligoi.[7]

One promising approach to signal detection based on recurrence plots focuses on the structure of the recurrence plot itself[8]. Essentially this approach starts with the recognition that the points in the recurrence plot for pure Gaussian noise are uniformly distributed (except for the diagonal) so that the existence of structured dark and light patterns must be due to a signal. This analysis develops various metrics to quantify these patterns and tests their performance in detecting signals.

This paper will present a different approach, based on the statistical properties of the points in the unthresholded recurrence plot. For a signal-in-noise data stream

consisting of M independent measurements the NxN unthresholded recurrence matrix is formed. This results in N(N-1)/2 data points as the recurrence matrix is symmetric about the diagonal. One potential advantage of recurrence-based detectors is therefore that the number of data points available for processing is increased from M to N(N-1)/2 points, where in practice N is nearly as large as M. Additionally, the time delay parameter used in constructing the recurrence plot explicitly incorporates the time information in the incoming signal. This information is not included in a normality detector. But, there is the disadvantage that there may be redundancies among the N(N-1)/2 data points now under consideration. If these redundancies are excessive, the additional data points will actually be detrimental rather than advantageous. Judicious choices for the embedding parameters of the recurrence matrix will minimize this problem.

In this paper, both the normality detector and recurrence-based detector are compared using a chi-squared test. For the normality detector, the M data points are used to construct a histogram, which is compared to the Gaussian distribution of the background noise in order to test the hypothesis of whether a signal is absent or present. The other detector, referred to as the recurrence plot detector, instead uses the N(N-1)/2 distances between data points in the recurrence matrix to construct a histogram which is compared to a Gamma-like distribution (derived in the text) of distances between the Gaussian-distributed noise vectors. The expected and observed distributions for both detectors are compared using a chi-squared test in order to determine the absence or presence of a signal.

Even though it has been shown[9] that the expectation of unthresholded recurrence plots can often be computed simply from second-order statistical quantities, this paper will directly address the question of whether the advantages (an increase in available data from M to N(N-1)/2 points and the inclusion of temporal correlations) are sufficient to evince low power signals for which the recurrence plot detector provides a performance gain over the normality detector.

The manuscript is organized as follows. First, there will be a brief explanation of recurrence plots, which introduces the mathematical notation for this paper. Next, the probability distributions relevant to this analysis will be derived. As the two detection approaches are formulated in detail, the importance of the precision required for the Gaussian distribution representing the background noise will be discussed, as well as binning techniques for the chi-squared test employed. Results are presented in the form of Receiver Operating Characteristic (ROC) curves for various signal types and parameter values for which the recurrence plot detector provides a detection performance gain are identified. Extensive calculations are required since the analysis is sensitive to several significant parameters; viz, sampling rate, embedding dimension, delay time, and a chi-squared statistics adjustment factor (to be defined in the text).

## *Recurrence Plots*

Recurrence plots were originally intended as a tool for analyzing the output of nonlinear, dynamical systems and have been used to estimate a host of quantities pertaining to the dimensionality and stability of the system being observed[3]. The goal in this work, however, is to use the recurrence plot as a tool for exploring correlations in time series data and not to draw inference about the system that produced the signal.

Consider the vector

$$\vec{x} = \{x(1), x(2), \ldots, x(m), \ldots x(M)\}$$

consisting of *M* real data values sampled at discrete times $t = m\Delta t$. From this single vector, a new family of *N* time-delay vectors each of length n<M is constructed by means of a *time delay embedding*

$$X_i = \{x(i), x(i+L), \ldots, x(i+(n-1)L)\} \quad i = 1, 2, \ldots, N$$

where *n* is referred to as the embedding dimension and *L* is a measure of time delay. Clearly *M=N+(n-1)L*. Hence the *M* one-dimensional data points have given rise to N vectors of dimension n. Prescriptions for selecting *L,n* can be found in[10], however, these approaches were designed for use with the output of a deterministic dynamical system subject to relatively low levels of noise. By contrast our application involves very high noise levels, thus the standard algorithms will fail. The approach used here, therefore, is to vary both L and n as parameters associated with the proposed detector.

The unthresholded recurrence matrix is the *N*x*N* matrix $[d_{i,j}]$ where

$$d_{i,j} = \left\| X_i - X_j \right\|$$

is the distance between the vectors $X_i$ and $X_j$. In this paper, this distance will always be the Euclidean distance; that is, the square root of the sums of the squares of the corresponding component differences. Other definitions of distance have been used in other applications. This unthresholded matrix will be the concept of interest in this paper.

Note that in the literature, a standard recurrence plot compares the distances to a pre-determined threshold value $\varepsilon$, and a black dot is placed at location (i,j) if $d_{i,j} \leq \varepsilon$ or a white dot if $d_{i,j} > \varepsilon$. So for any threshold $\varepsilon \geq 0$, the main diagonal of the recurrence plot will always be black. By convention, the (1,1) location is the lower left entry of the recurrence plot and the (*N, N*) location is in the upper right corner. Mathematically, the entries of the recurrence plot are given by

4

$$\Theta\left(\varepsilon - \left\| X_i - X_j \right\|\right)$$

where $\Theta$ is the Heaviside step function

$$\Theta(z) = \begin{cases} 1 & z \geq 0 \\ 0 & z < 0 \end{cases}$$

so a value of 1 corresponds to a black dot, and 0 to a white dot.

Consider the following simple example. Suppose the original data vector is $\vec{x} = \{0, 4, 2, 3, 7, 9\}$ and let $n=3$ and $L=1$. Then $N=6-(2\mathrm{x}1)=4$ and

$$X_1 = \{0, 4, 2\}$$
$$X_2 = \{4, 2, 3\}$$
$$X_3 = \{2, 3, 7\}$$
$$X_4 = \{3, 7, 9\}$$

The unthresholded recurrence plot is then given by

$$[d_{i,j}] = \begin{bmatrix} \sqrt{67} & \sqrt{62} & \sqrt{21} & 0 \\ \sqrt{30} & \sqrt{21} & 0 & \sqrt{21} \\ \sqrt{21} & 0 & \sqrt{21} & \sqrt{62} \\ 0 & \sqrt{21} & \sqrt{30} & \sqrt{67} \end{bmatrix}$$

Note that in this example the time delay vectors are all distinct, but there are clearly redundancies in the distance values.

Standard recurrence plots have been useful in many applications because they provide evidence of the underlying structure of a system. For example, compare the recurrence plots for a deterministic periodic function, a chaotic system, and random noise in Fig. (1).
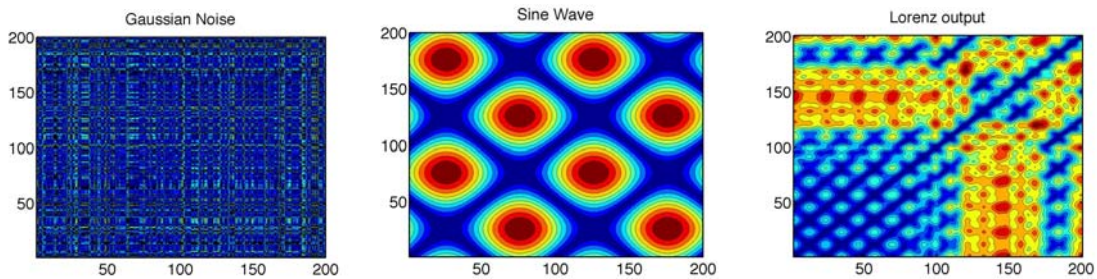


**Fig. 1.** Example unthresholded recurrence plots for Gaussian noise, a sine-wave, and the output of the chaotic Lorenz system.

5

## *Probability Distributions*

In order to formulate the signal detection strategies to be assessed in this paper, some basic probability distributions need to be calculated. In these derivations, $x_1, x_2, \ldots, x_n$ are defined to be independent Gaussian random variables, each with zero mean and variance $\sigma^2$. The $x_i$ used here are arbitrary random variables and are not related to the $X_i$ defined already as the delay vectors. Additionally, the index $n$ is not necessarily related to the embedding dimension although later it will be interpreted as such. For the purposes of our analysis, we require the probability distribution of the length and the length squared of the vector $(x_1, x_2, \ldots, x_n)$. Each $x_i$ has probability density function

$$p(x_i) = \frac{1}{\sigma\sqrt{2\pi}} e^{-x_i^2/2\sigma^2} \quad i = 1, 2, \ldots, n.$$

We first derive the probability density function for $r = \sqrt{x_1^2 + x_2^2 + \cdots + x_n^2}$. This can be achieved readily if we can obtain a one-to-one transformation on $R^n$ in which $r$ is one of the transformed variables and $r$ is also separable from the other variables in the joint probability density function of the transformed variables. A transformation of variables $(x_1, x_2, \ldots, x_n) \rightarrow (r, \theta_1, \ldots, \theta_{n-1})$ satisfying these requirements is given by

$$x_1 = r \cos \theta_1$$
$$x_2 = r \sin \theta_1 \cos \theta_2$$
$$x_3 = r \sin \theta_1 \sin \theta_2 \cos \theta_3$$
$$\vdots$$
$$x_{n-1} = r \sin \theta_1 \sin \theta_2 \ldots \sin \theta_{n-2} \cos \theta_{n-1}$$
$$x_n = r \sin \theta_1 \sin \theta_2 \ldots \sin \theta_{n-2} \sin \theta_{n-1}$$

where $0 \leq r < \infty$ and $0 \leq \theta_i < \pi$. Then

$$p(r, \theta_1, \ldots \theta_{n-1}) = J_n \prod_{i=1}^{n} p(x_i)$$

where $J_n$ is the Jacobian of the transformation. Inserting the formula for $J_n$ computed in Appendix A yields

$$p(r, \theta_1, \ldots, \theta_{n-1}) = r^{n-1} (\sin \theta_1)^{n-2} (\sin \theta_2)^{n-3} \ldots \sin \theta_{n-2} \frac{1}{\sigma^n} \left( \frac{1}{2\pi} \right)^{\frac{n}{2}} e^{-r^2/2\sigma^2}$$

The terms containing $\theta_1, \ldots, \theta_{n-1}$ may be integrated out to get $p(r)$, but, since they are all independent of $r$, they must be a constant. It is easier to simply note that

6

$$p(r) = C r^{n-1} e^{-r^2/2\sigma^2}$$

where

$$C = \left( \int_0^\infty r^{n-1} e^{-r^2/2\sigma^2} dr \right)^{-1}$$

since a probability density function must integrate to one. Now

$$\int_0^\infty r^{n-1} e^{-r^2/2\sigma^2} dr = \frac{\Gamma\left(\dfrac{n}{2}\right)}{2\left(\dfrac{1}{2\sigma^2}\right)^{n/2}}$$

so

$$C = \frac{2\left(\dfrac{1}{2}\right)^{n/2}}{\sigma^n \Gamma\left(\dfrac{n}{2}\right)}$$

and

$$p(r) = \frac{2\left(\dfrac{1}{2}\right)^{n/2}}{\sigma^n \Gamma\left(\dfrac{n}{2}\right)} r^{n-1} e^{-r^2/2\sigma^2} \quad 0 \le r < \infty \tag{1}$$

where $\Gamma(\cdot)$ is the Gamma function. This is the probability density function of the Euclidean length of n-dimensional vectors in $R^n$ whose components are i.i.d and drawn from a zero mean Gaussian random process with variance $\sigma^2$. The mean of the above distribution is given by

7

$$\mu_r = \int_0^{\infty} r p(r)\, dr$$

$$= \frac{2\left(\dfrac{1}{2}\right)^{n/2}}{\sigma^n \Gamma\left(\dfrac{n}{2}\right)} \int_0^{\infty} r^n e^{-r^2/2\sigma^2}\, dr$$

$$= \frac{2\left(\dfrac{1}{2}\right)^{n/2}}{\sigma^n \Gamma\left(\dfrac{n}{2}\right)} \frac{\Gamma\left(\dfrac{n+1}{2}\right)}{2\left(\dfrac{1}{2\sigma^2}\right)^{\frac{n+1}{2}}}$$

$$= \frac{\sqrt{2}\,\Gamma\left(\dfrac{n+1}{2}\right)}{\Gamma\left(\dfrac{n}{2}\right)}\sigma$$

and the variance by

$$\sigma_r^2 = \int_0^{\infty} r^2 p(r)\, dr - \mu_r^2$$

$$= \frac{2\left(\dfrac{1}{2}\right)^{n/2}}{\sigma^n \Gamma\left(\dfrac{n}{2}\right)} \int_0^{\infty} r^{n+1} e^{-r^2/2\sigma^2}\, dr - \mu_r^2$$

$$= \frac{2\left(\dfrac{1}{2}\right)^{n/2}}{\sigma^n \Gamma\left(\dfrac{n}{2}\right)} \frac{\Gamma\left(\dfrac{n}{2}+1\right)}{2\left(\dfrac{1}{2\sigma^2}\right)^{n/2+1}} - \mu_r^2$$

$$= n\sigma^2 - 2\left(\frac{\Gamma\left(\dfrac{n+1}{2}\right)}{\Gamma\left(\dfrac{n}{2}\right)}\right)^2 \sigma^2$$

$$= \left[ n - 2\left(\frac{\Gamma\left(\dfrac{n+1}{2}\right)}{\Gamma\left(\dfrac{n}{2}\right)}\right)^2 \right] \sigma^2$$

Note that in the special case where n=3, these formulas reduce to

$$p(r) = \frac{1}{\sigma^3}\sqrt{\frac{2}{\pi}}r^2 e^{-r^2/2\sigma^2} \quad 0 \le r < \infty$$

$$\mu_r = 2\sqrt{\frac{2}{\pi}}\sigma$$

$$\sigma_r^2 = \left(3 - \frac{8}{\pi}\right)\sigma^2$$

Next we derive the distribution of $r^2 = x_1^2 + x_2^2 + \cdots x_n^2$. Making the change of variables $u=r^2$ yields

$$p(u) = \frac{p(r(u))}{\left|\dfrac{du}{dr}\right|}$$

$$= \frac{2\left(\dfrac{1}{2}\right)^{n/2}}{\sigma^n \Gamma\left(\dfrac{n}{2}\right)}\frac{u^{(n-1)/2}e^{-u/2\sigma^2}}{2u^{1/2}}$$

$$= \frac{\left(\dfrac{1}{2}\right)^{n/2}}{\sigma^n \Gamma\left(\dfrac{n}{2}\right)}u^{n/2-1}e^{-u/2\sigma^2} \quad 0 \le u < \infty \tag{2}$$

This distribution is readily recognized as a Gamma distribution, or more particularly, a Chi-square distribution with n degrees of freedom when $\sigma = 1$. For this distribution, the mean is given by

$$\mu_u = \int_0^\infty u\, p(u)\, du$$

$$= \frac{\left(\dfrac{1}{2}\right)^{n/2}}{\sigma^n \Gamma\left(\dfrac{n}{2}\right)}\int_0^\infty u^{n/2}e^{-u/2\sigma^2}\, du$$

$$= \frac{\left(\dfrac{1}{2}\right)^{n/2}}{\sigma^n \Gamma\left(\dfrac{n}{2}\right)}\frac{\Gamma\left(\dfrac{n}{2}+1\right)}{\left(\dfrac{1}{2\sigma^2}\right)^{n/2+1}}$$

$$= n\sigma^2$$

and the variance by

$$\sigma_u^2 = \int_0^\infty u^2 p(u)\, du - \mu_u^2$$

$$= \frac{\left(\dfrac{1}{2}\right)^{n/2}}{\sigma^n \Gamma\left(\dfrac{n}{2}\right)} \int_0^\infty u^{n/2+1} e^{-u/2\sigma^2}\, du - \mu_u^2$$

$$= \frac{\left(\dfrac{1}{2}\right)^{n/2}}{\sigma^n \Gamma\left(\dfrac{n}{2}\right)} \frac{\Gamma\left(\dfrac{n}{2}+2\right)}{\left(\dfrac{1}{2\sigma^2}\right)^{n/2+2}} - n^2\sigma^4$$

$$= n(n+2)\sigma^4 - n^2\sigma^4 = 2n\sigma^4$$

In the special case where $n = 3$, these formulas become

$$p(u) = \frac{1}{\sigma^3\sqrt{2\pi}} u^{1/2} e^{-u/2\sigma^2} \quad 0 \le u < \infty$$

$$\mu_u = 3\sigma^2$$

$$\sigma_u^2 = 6\sigma^4$$

The formulas derived above can be found in the literature; for example, a proof for (1) by means of a geometrical method may be found in Parzen[11] and a proof for (2) by means of characteristic functions is in McDonough and Whelan[1]. In fact, the case for $n = 2$ and 3 is found in many textbooks as an example of the transformation of variables. The straightforward proof by induction given here is included because the authors have not seen it in the literature.

Formulas (1) and (2) give the probability densities of the length and the length squared for a vector whose components are independent samples from the same Gaussian distribution with mean 0 and variance $\sigma^2$. However, what is needed for this paper is the distance between two vectors. That is, let $x_1,x_2,\ldots,x_n$ and $y_1,y_2,\ldots,y_n$ be independent random variables chosen from the same Gaussian distribution with mean 0 and variance $\sigma^2$, and define

$$r = \sqrt{(x_1 - y_1)^2 + (x_2 - y_2)^2 + \cdots + (x_n - y_n)^2} \quad \text{and}$$

$$u = r^2$$

However, note that if x and y are independent Gaussian random variables with mean 0 and variance $\sigma^2$, then *(x-y)* is also Gaussian, again with mean 0 but now with variance $2\sigma^2$. In fact, we can relax the requirement that x and y have zero mean. As long as they have the same mean, then the result is equally valid. Consequently, for the case of the distance between two vectors, formulas (1) and (2) become

$$p(r) = \frac{2\left(\dfrac{1}{4}\right)^{n/2}}{\sigma^n \Gamma\left(\dfrac{n}{2}\right)} r^{n-1} e^{-r^2/4\sigma^2} \quad 0 \le r < \infty \tag{3}$$

$$p(u) = \frac{\left(\dfrac{1}{4}\right)^{n/2}}{\sigma^n \Gamma\left(\dfrac{n}{2}\right)} u^{n/2-1} e^{-u/4\sigma^2} \quad 0 \le u < \infty \tag{4}$$

## Detection Strategies

Suppose we are sampling from a data stream of values of the form

$$x(m) = s(m) + n(m) \qquad m = 1, 2, \ldots, M$$

where the $s(m)$ are values of a signal and the $n(m)$ are Gaussian white noise with zero mean and variance $\sigma^2$. The signal may or may not be present, and the parameters of the signal are unknown. Two approaches will be evaluated in this paper: the first is a straightforward normality detector and the second makes use of the recurrence matrix of the data.

### *Normality Detector*

If the signal is absent, then the measured values $x(m)$ represent just Gaussian noise $n(m)$. Hence the histogram generated from the $x(m)$ values should fit the Gaussian density function of the background noise. This hypothesis is tested by means of a $\chi^2$ Goodness-of-fit test based on the $\chi^2$ statistic

$$S = \sum_{k=1}^{K} \frac{(o_k - e_k)^2}{e_k}$$

where $K$ is the number of bins of the histogram and the $o_k$ and $e_k$ are the observed counts and the expected Gaussian counts in each bin, respectively. The statistic $S$ is compared to the appropriate threshold value $\chi_0^2$ of the $\chi^2$ distribution with $K$-1 degrees of freedom. If

$S \le \chi_0^2$ then we declare no signal present. However, if $S > \chi_0^2$, then we declare a signal present.

In the calculations to follow, $K=15$ bins proved to be suitable for $M=100$ to $200$ (the size of the signals considered in this work). The threshold used in this detection scheme corresponded to a critical region of size 0.05 for the $\chi^2$ distribution.

Initially the Gaussian noise was generated using the MATLAB random number generator. It was surprising how often (approximately 5% of the time) such values failed the $\chi^2$ test for normality. A typical example is shown in Figure 2. Note the
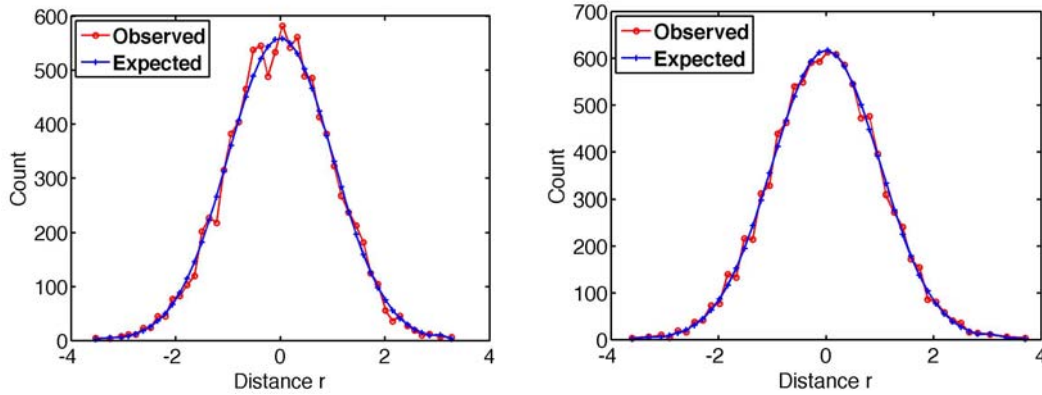


**Fig. 2.** Comparison of MATLAB generated Gaussian deviates (left) and those generated from the "ideal" Gaussian (right). The estimated distribution in the left plot fails the chi-squared test for normality despite the fact that the data was produced by a Gaussian number generator.

frequent presence of spikes near the mean of the plot. Such anomalies cannot be tolerated in testing our technique because these spikes produce false alarms. For detection of very small signals, a much more precise representation of the background Gaussian noise is needed, so we developed a method for constructing data sets having a nearly ideal normal properties [Appendix C].

## *Recurrence Plot Detector*

In this case, the time-delay vectors $X_i$ for $i = 1,...,N$ are constructed from the $x(m)$ values as described before, thus incorporating the time signature of the original time series. Each of these vectors has length $n$, where $n$ is the embedding dimension, and each component of $X_i$ is a value in the original data stream which samples are assumed to be independent. The $N$x$N$ unthresholded recurrence plot has entries

$$d_{i,j} = \left\| X_i - X_j \right\|$$

which is just the distance r between the vectors as described above. If there is no signal present then the original samples come from a Gaussian distribution with zero mean and variance $\sigma^2$ and so the non-diagonal entries in the unthresholded recurrence plot follow the Gamma-like distribution given in Equation (3). To avoid duplications, we only use the $N(N-1)/2$ entries above the main diagonal. This technique could also be based on $r^2$ values, and then Equation (4) would be used.

The procedure is now similar to the first technique. If there is no signal present, the histogram of the $d_{i,j}$ values should fit the Gamma-like distribution of Equation (3). Again a $\chi^2$ Goodness-of-fit test can be applied with a threshold based on the $\chi^2$ distribution with $K$-1 degrees of freedom if $\sigma$ is known ($K$-2 degrees of freedom if $\sigma$ is estimated from the data)

We now have many more data points than in the corresponding Normality Detector Test, but $K=15$ bins still proved to be sufficient for a valid $\chi^2$ test. Again, if the $\chi^2$ value was below the threshold, we declared the signal to be absent; if above the threshold, we declared the signal present. In this case, however, we found that for the types of signals treated in this analysis, too many false positives occurred when comparing $S$ to the threshold $\chi_o^2$ . That is, the value of $S$ was often rather large even with no signal present, but much larger when the signal was present. This effect is probably due to the redundancies in the recurrence matrix data. The derivation of the null distribution assumed independent distances when in reality these distances may contain redundancies. The result is that the size of the test (the probability that the null hypothesis is rejected) is not commensurate with the observed Type-I error. In this case, if the threshold $\chi_o^2$ is set such that we expect 5% false alarms, the correlations in the data result in a percentage of rejections that can be much larger than 5%. We therefore calibrated our test by using an adjustment factor $\kappa$ to multiply the $\chi^2$ statistic, $S$. This factor reduces the number of false positives to the correct level thus allowing for a more meaningful test[12]. Calculations have shown that small values $n=2,3,4$ of the embedding dimension work best in this detector, and for these values $\kappa=0.5,0.3,0.1$ respectively. The number of data can also influence the choice of $\kappa$. We have found that larger values for $M$ require a decrease in $\kappa$ value.

Embedding dimension n is one important sensitivity parameter; others are the delay time, $L$ and the sampling rate of the original data stream. Of course it is desirable that our detection technique will be effective for many signal types. The optimal values of the key sensitivity parameters will generally be a function of the type of signal received. Consequently, in practice, a bank of parameter values should be swept through to test for the presence of an unknown signal.

Both detectors (normality and recurrence) are compared here in terms of their Receiver Operating Characteristic (ROC) performance. The ROC curve simply displays the probability of detection $P_D$ versus the probability of false alarm $P_{fa}$ associated with these detectors as a function of the detection threshold. The signal of interest was taken to be a 10Hz sine wave with additive Gaussian noise. The signal-to-noise ratio (SNR) was taken as the average power of the signal divided by the variance of the noise. Figure

(3) shows some typical results comparing detector performance as a function of signal to noise ratio.
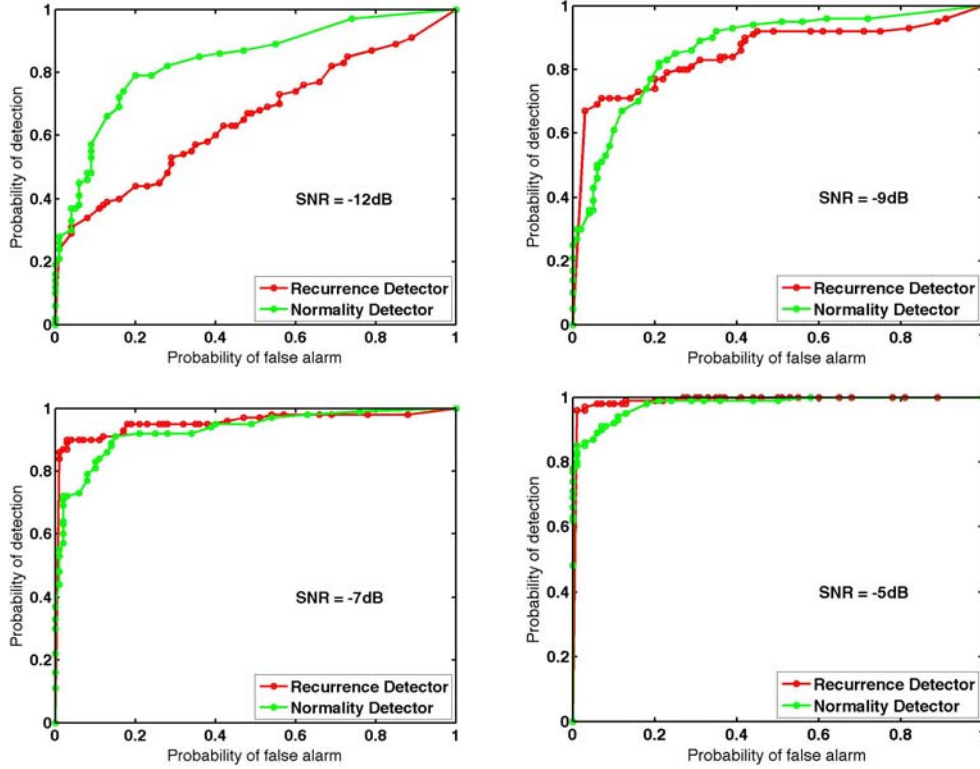


**Fig. 3.** ROC curves associated with detecting a 10 Hz. sine-wave in Gaussian noise for varying SNR levels. Sampling parameters were $M$=100 and $\Delta t$=0.01s. Embedding parameters were $n$=3, $L$=5. Threshold factor was $\kappa$=0.3.

The embedding parameters used in this example were $M$=100, $n$=3, $L$=5. The signal was sampled at intervals of $\Delta t$=0.01s. For the recurrence-based detector the threshold adjustment factor was set to $\kappa$=0.3. The results of Figure (3) are typical of those found using other embedding parameters. For low SNR values, the normality detector easily outperforms the recurrence detector. However, for intermediate SNR levels there typically exists a range where the recurrence-based detector shows superior ROC performance. Changing the embedding parameters does not seem to affect the result. For example, using a dimension of $n$=2 and $L$=8 and $\kappa$=0.5 results in the ROC curves of Fig (4).

Again, for low SNR values (<10dB) the chi-square test for non-normality is the best performer while for higher SNR values the recurrence-based detector shows the best ROC performance. The influence of the number of points and sampling rate were also
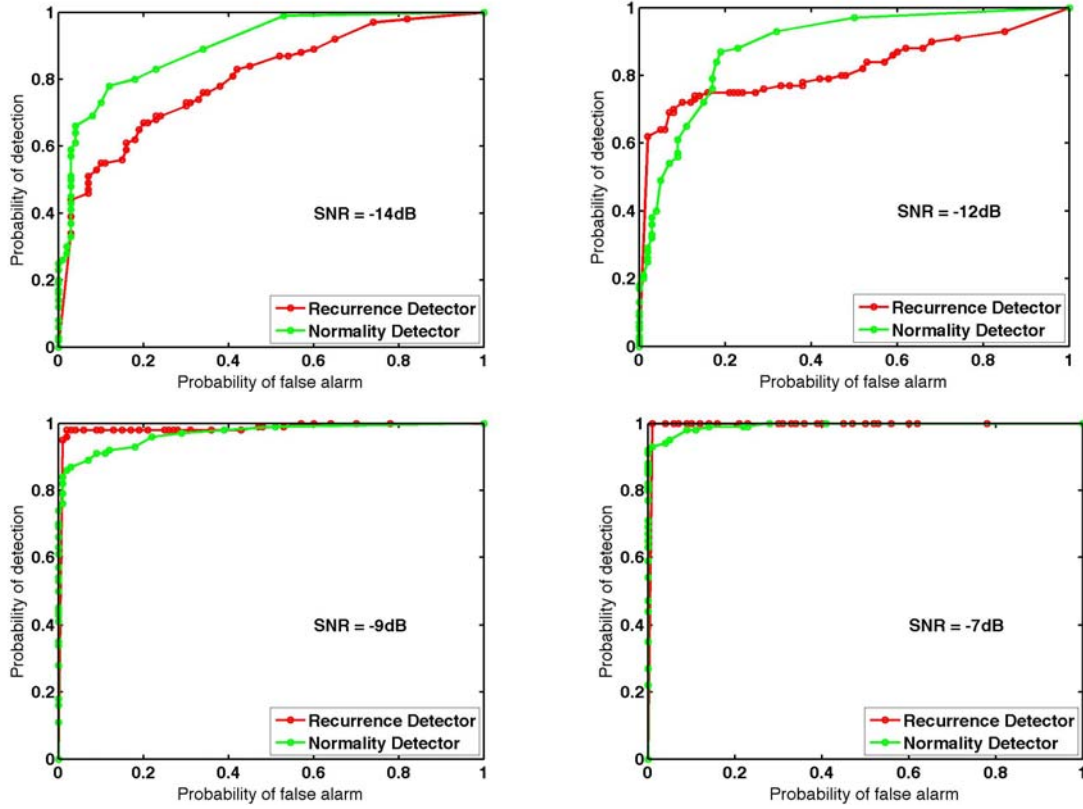
14
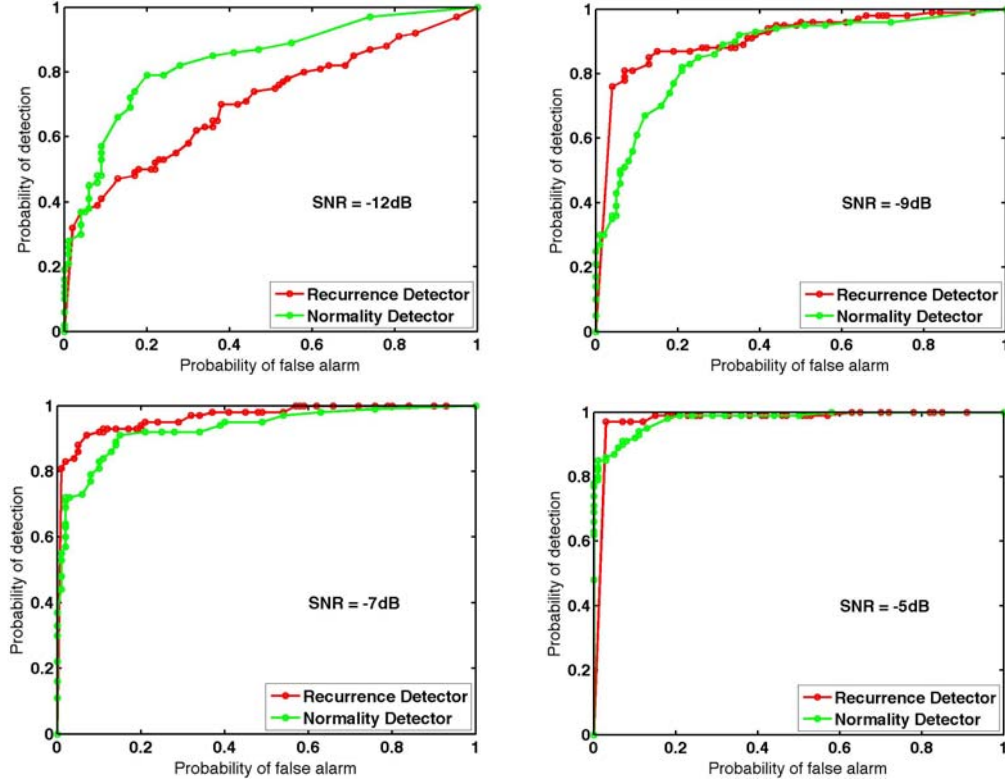
***Fig. 4***. ROC curves associated with detecting a 10 Hz. sine-wave in Gaussian noise for varying SNR levels. Sampling parameters were *M = 100* and *Δt = 0.01s*. Embedding parameters were *n = 2, L = 8*. Threshold factor was *κ = 0.5*.

explored. Fig (5) shows the results of increasing the number of data to *M =200* points and decreasing the sampling interval to *Δt = 0.005s* (thus the total duration of the signal is kept constant from the previous examples). The embedding parameters used were *n = 2, L = 8* as in the previous example. For this number of data, an appropriate threshold value was determined to be *κ = 0.3*.

As before there exists a range of SNR values below which the normality detector yields the more powerful result. Above -12dB SNR, however, the recurrence-based detector again shows superior performance until both methods converge to unity for the probability of detection for any probability of false alarm.

The results shown above hold for a variety of both embedding and sampling parameters. For *n>3*, however, the redundancies in the recurrence plot become much larger so that the threshold adjustment factor must be set to values *κ<0.1*. It is therefore apparent that there does exist a range of SNR values for which the recurrence-based

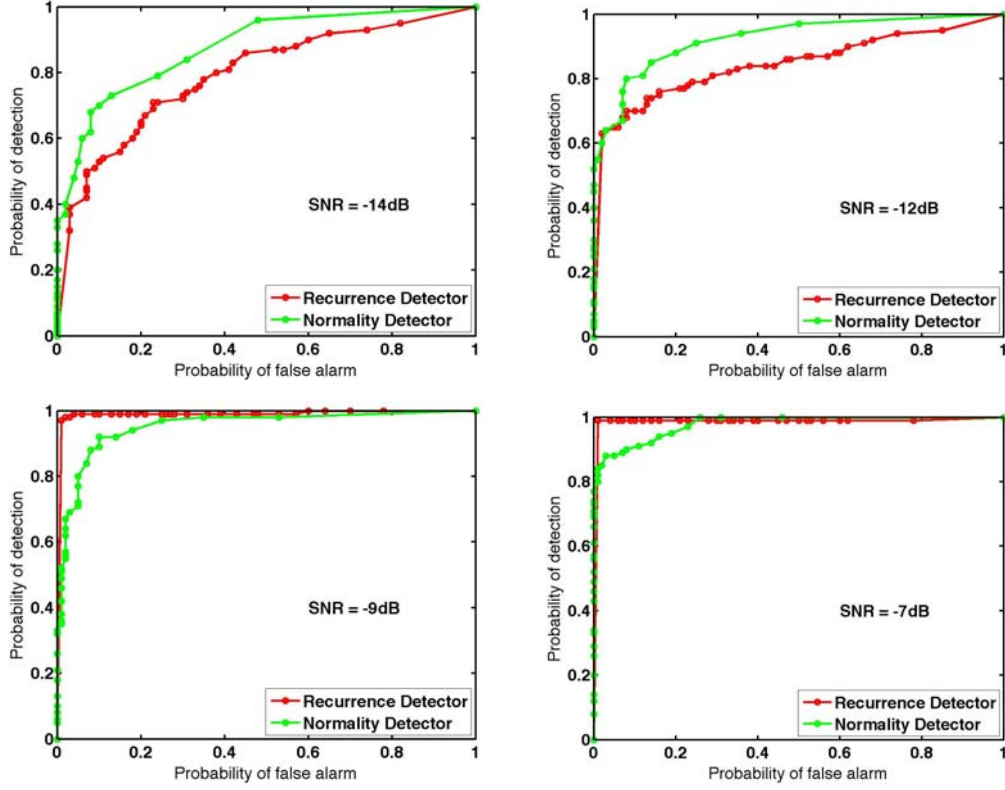*Fig. 5.* ROC curves associated with detecting a 10 Hz. sine-wave in Gaussian noise for varying SNR levels. Sampling parameters were *M*=200 and Δt=0.005s. Embedding parameters were *n*=2, *L*=8. Threshold factor was κ=0.3.

detection schemes have some merit over the more general normality detector in detecting the presence of a sine-wave in Gaussian noise. It should be stressed, however, that the value of these detectors is that they do not assume a priori knowledge of the incoming signal. If it was known that a sine-wave was the signal of interest an optimal detector can be derived, depending on how much is known about the sine-wave (frequency, phase, etc.).

As another test of the recurrence-based detector, the detection of a square wave in additive Gaussian noise was considered. The embedding parameters *n = 2*, and *L = 8* were used along with the sampling parameters of *M = 200, Δt = 0.01*. Figure (6) shows these results.

Even for a very different type of signal, the same trend in ROC curves persists as a function of SNR.

*Fig. 6.* ROC curves associated with detecting a 10 Hz. square-wave in Gaussian noise for varying SNR levels. Sampling parameters were *M = 100 and Δt = 0.01s*. Embedding parameters were *n = 2, L = 8*. Threshold factor was *κ = 0.3*.

# Summary

This work has focused on the detection of signals in noise using a detector based on the signal's recurrence matrix. Under the null hypothesis of no signal, the probability distribution for the entries of the recurrence matrix was derived and found to be a Gamma-like distribution. Using this distribution, a chi-squared test was performed in order to assess whether or not some underlying signal was present. Due to redundancies in the recurrence plot, this test had to be slightly modified in order to produce a meaningful Type-I error. Receiver Operating Characteristic (ROC) curves were then used to assess the performance of this detector as a function of embedding parameters, signal sampling parameters, and signal-to-noise ratio (SNR). Comparisons were drawn between the recurrence-based detector and a normality detector for demonstrating non-normality of the incoming signal. Results indicated that there is a range of SNR values for which the recurrence-based detector offers superior performance (in the sense of lower Type-II error for a given Type-I error) over the normality detector. This behavior was observed for both sine wave and square wave signals in additive Gaussian noise.

# Appendix A.

**Calculation of the Jacobian of the Transformation of Variables**.

For the transformation of variables $(x_1, x_2, \ldots, x_n) \rightarrow (r, \theta_1, \ldots, \theta_{n-1})$

$$x_1 = r\cos\theta_1$$
$$x_2 = r\sin\theta_1\cos\theta_2$$
$$x_3 = r\sin\theta_1\sin\theta_2\cos\theta_3$$
$$\vdots$$
$$x_{n-1} = r\sin\theta_1\sin\theta_2\ldots\sin\theta_{n-2}\cos\theta_{n-1}$$
$$x_n = r\sin\theta_1\sin\theta_2\ldots\sin\theta_{n-2}\sin\theta_{n-1}$$

where $0 \leq r < \infty$ and $0 \leq \theta_i < \pi$, the Jacobian is given by

$$J_n = \begin{vmatrix} \cos\theta_1 & -r\sin\theta_1 & 0 & 0 & \ldots & 0 \\ \sin\theta_1\cos\theta_2 & r\cos\theta_1\cos\theta_2 & -r\sin\theta_1\sin\theta_2 & 0 & \ldots & 0 \\ \sin\theta_1\sin\theta_2\cos\theta_3 & r\cos\theta_1\sin\theta_2\cos\theta_3 & r\sin\theta_1\cos\theta_2\cos\theta_3 & -r\sin\theta_1\sin\theta_2\sin\theta_3 & \ldots & 0 \\ \vdots & \vdots & \vdots & \ddots & & \vdots \\ \sin\theta_1\sin\theta_2\ldots\sin\theta_{n-2}\cos\theta_{n-1} & r\cos\theta_1\sin\theta_2\ldots\sin\theta_{n-2}\cos\theta_{n-1} & r\sin\theta_1\cos\theta_2\ldots\sin\theta_{n-2}\cos\theta_{n-1} & \ldots & \ldots & -r\sin\theta_1\ldots\sin\theta_{n-2}\sin\theta_{n-1} \\ \sin\theta_1\ldots\sin\theta_{n-1} & r\cos\theta_1\sin\theta_2\ldots\sin\theta_{n-1} & r\sin\theta_1\cos\theta_2\ldots\sin\theta_{n-1} & \ldots & \ldots & r\sin\theta_1\sin\theta_2\ldots\sin\theta_{n-2}\cos\theta_{n-1} \end{vmatrix}$$

we shall prove that

$$J_n = r^{n-1}\left(\sin\theta_1\right)^{n-2}\left(\sin\theta_2\right)^{n-3}\ldots\sin\theta_{n-2}$$

Consider $J_n$ for a few special cases:

For $n = 2$:

$$J_2 = \begin{vmatrix} \cos\theta_1 & -r\sin\theta_1 \\ \sin\theta_1 & r\cos\theta_1 \end{vmatrix} = r$$

For $n = 3$: by expanding by cofactors of the first row

$$J_3 = \begin{vmatrix} \cos\theta_1 & -r\sin\theta_1 & 0 \\ \sin\theta_1\cos\theta_2 & r\cos\theta_1\cos\theta_2 & -r\sin\theta_1\sin\theta_2 \\ \sin\theta_1\sin\theta_2 & r\cos\theta_1\sin\theta_2 & r\sin\theta_1\cos\theta_2 \end{vmatrix}$$

$$= \cos\theta_1 r^2\sin\theta_1\cos\theta_1 + r\sin\theta_1 r\sin^2\theta_1 = r^2\sin\theta_1$$

For $n = 4$: by expanding by cofactors of the first row

$$J_4 = \begin{vmatrix} \cos\theta_1 & -r\sin\theta_1 & 0 & 0 \\ \sin\theta_1\cos\theta_2 & r\cos\theta_1\cos\theta_2 & -r\sin\theta_1\sin\theta_2 & 0 \\ \sin\theta_1\sin\theta_2\cos\theta_3 & r\cos\theta_1\sin\theta_2\cos\theta_3 & r\sin\theta_1\cos\theta_2\cos\theta_3 & -r\sin\theta_1\sin\theta_2\sin\theta_3 \\ \sin\theta_1\sin\theta_2\sin\theta_3 & r\cos\theta_1\sin\theta_2\sin\theta_3 & r\sin\theta_1\cos\theta_2\sin\theta_3 & r\sin\theta_1\sin\theta_2\cos\theta_3 \end{vmatrix}$$

$$= \cos\theta_1 \begin{vmatrix} r\cos\theta_1\cos\theta_2 & -r\sin\theta_1\sin\theta_2 & 0 \\ r\cos\theta_1\sin\theta_2\cos\theta_3 & r\sin\theta_1\cos\theta_2\cos\theta_3 & -r\sin\theta_1\sin\theta_2\sin\theta_3 \\ r\cos\theta_1\sin\theta_2\sin\theta_3 & r\sin\theta_1\cos\theta_2\sin\theta_3 & r\sin\theta_1\sin\theta_2\cos\theta_3 \end{vmatrix}$$

$$+ r\sin\theta_1 \begin{vmatrix} \sin\theta_1\cos\theta_2 & -r\sin\theta_1\sin\theta_2 & 0 \\ \sin\theta_1\sin\theta_2\cos\theta_3 & r\sin\theta_1\cos\theta_2\cos\theta_3 & -r\sin\theta_1\sin\theta_2\sin\theta_3 \\ \sin\theta_1\sin\theta_2\sin\theta_3 & r\sin\theta_1\cos\theta_2\sin\theta_3 & r\sin\theta_1\sin\theta_2\cos\theta_3 \end{vmatrix}$$

$$= \cos\theta_1(r\cos\theta_1)(\sin\theta_1)(\sin\theta_1) \begin{vmatrix} \cos\theta_2 & -r\sin\theta_2 & 0 \\ \sin\theta_2\cos\theta_3 & r\cos\theta_2\cos\theta_3 & -r\sin\theta_2\sin\theta_3 \\ \sin\theta_2\sin\theta_3 & r\cos\theta_2\sin\theta_3 & r\sin\theta_2\cos\theta_3 \end{vmatrix}$$

$$+ r\sin\theta_1(\sin\theta_1)(\sin\theta_1)(\sin\theta_1) \begin{vmatrix} \cos\theta_2 & -r\sin\theta_2 & 0 \\ \sin\theta_2\cos\theta_3 & r\cos\theta_2\cos\theta_3 & -r\sin\theta_2\sin\theta_3 \\ \sin\theta_2\sin\theta_3 & r\cos\theta_2\sin\theta_3 & r\sin\theta_2\cos\theta_3 \end{vmatrix}$$

$$= \left( r\sin^2\theta_1\cos^2\theta_1 + r\sin^2\theta_1\sin^2\theta_1 \right) J_3$$

$$= r\sin^2\theta_1 r^2\sin\theta_2 = r^3\sin^2\theta_1\sin\theta_2$$

In general we will demonstrate that

$$J_n(r,\theta_1,\theta_2,\ldots,\theta_{n-1}) = r^{n-1}(\sin\theta_1)^{n-2}(\sin\theta_2)^{n-3}\ldots\sin\theta_{n-2}$$

The proof is by induction and again proceeds by expanding by cofactors of the first row. We have shown it above for $n = 2,3,4$. Assume true for $n = (K-1)$. Then

$$J_K\left(r,\theta_1,\ldots,\theta_{K-1}\right) =$$

$$\begin{vmatrix}
\cos\theta_1 & -r\sin\theta_1 & 0 & 0 & \cdots & 0 \\
\sin\theta_1\cos\theta_2 & r\cos\theta_1\cos\theta_2 & -r\sin\theta_1\sin\theta_2 & 0 & \cdots & 0 \\
\sin\theta_1\sin\theta_2\cos\theta_3 & r\cos\theta_1\sin\theta_2\cos\theta_3 & r\sin\theta_1\cos\theta_2\cos\theta_3 & -r\sin\theta_1\sin\theta_2\sin\theta_3 & \cdots & 0 \\
\vdots & \vdots & \vdots & & \ddots & \vdots \\
\sin\theta_1\sin\theta_2\ldots\sin\theta_{K-2}\cos\theta_{K-1} & r\cos\theta_1\sin\theta_2\ldots\sin\theta_{K-2}\cos\theta_{K-1} & r\sin\theta_1\cos\theta_2\ldots\sin\theta_{K-2}\cos\theta_{K-1} & \cdots & \cdots & -r\sin\theta_1\ldots\sin\theta_{K-2}\sin\theta_{K-1} \\
\sin\theta_1\ldots\sin\theta_{K-1} & r\cos\theta_1\sin\theta_2\ldots\sin\theta_{K-1} & r\sin\theta_1\cos\theta_2\ldots\sin\theta_{K-1} & \cdots & \cdots & r\sin\theta_1\sin\theta_2\ldots\sin\theta_{K-2}\cos\theta_{K-1}
\end{vmatrix}$$

$$= \cos\theta_1 \begin{vmatrix}
r\cos\theta_1\cos\theta_2 & -r\sin\theta_1\sin\theta_2 & \cdots & 0 \\
r\cos\theta_1\sin\theta_2\cos\theta_3 & r\sin\theta_1\cos\theta_2\cos\theta_3 & \cdots & 0 \\
\vdots & \vdots & \ddots & \vdots \\
r\cos\theta_1\sin\theta_2\ldots\sin\theta_{K-2}\cos\theta_{K-1} & r\sin\theta_1\cos\theta_2\ldots\sin\theta_{K-2}\cos\theta_{K-1} & \cdots & -r\sin\theta_1\ldots\sin\theta_{K-2}\sin\theta_{K-1} \\
r\cos\theta_1\sin\theta_2\ldots\sin\theta_{K-2}\sin\theta_{K-1} & r\sin\theta_1\cos\theta_2\ldots\sin\theta_{K-2}\sin\theta_{K-1} & \cdots & r\sin\theta_1\ldots\sin\theta_{K-2}\cos\theta_{K-1}
\end{vmatrix}$$

$$+r\sin\theta_1 \begin{vmatrix}
\sin\theta_1\cos\theta_2 & -r\sin\theta_1\sin\theta_2 & \cdots & 0 \\
\sin\theta_1\sin\theta_2\cos\theta_3 & r\sin\theta_1\cos\theta_2\cos\theta_3 & \cdots & 0 \\
\vdots & \vdots & \ddots & \vdots \\
\sin\theta_1\ldots\sin\theta_{K-2}\cos\theta_{K-1} & r\sin\theta_1\cos\theta_2\ldots\sin\theta_{K-2}\cos\theta_{K-1} & \cdots & -r\sin\theta_1\ldots\sin\theta_{K-2}\sin\theta_{K-1} \\
\sin\theta_1\ldots\sin\theta_{K-2}\sin\theta_{K-1} & r\sin\theta_1\cos\theta_2\ldots\sin\theta_{K-2}\sin\theta_{K-1} & \cdots & r\sin\theta_1\ldots\sin\theta_{K-2}\cos\theta_{K-1}
\end{vmatrix}$$

$$= \cos\theta_1\left(r\cos\theta_1\right)\left(\sin\theta_1\right)^{K-2} \begin{vmatrix}
\cos\theta_2 & -r\sin\theta_2 & \cdots & 0 \\
\sin\theta_2\cos\theta_3 & r\cos\theta_2\cos\theta_3 & \cdots & 0 \\
\vdots & \vdots & \ddots & \vdots \\
\sin\theta_2\ldots\sin\theta_{K-2}\cos\theta_{K-1} & r\cos\theta_2\ldots\sin\theta_{K-2}\cos\theta_{K-1} & \cdots & -r\sin\theta_2\ldots\sin\theta_{K-2}\sin\theta_{K-1} \\
\sin\theta_2\ldots\sin\theta_{K-2}\sin\theta_{K-1} & r\cos\theta_2\ldots\sin\theta_{K-2}\sin\theta_{K-1} & \cdots & r\sin\theta_2\ldots\sin\theta_{K-2}\cos\theta_{K-1}
\end{vmatrix}$$

$$+r\sin\theta_1\left(\sin\theta_1\right)^{K-1} \begin{vmatrix}
\cos\theta_2 & -r\sin\theta_2 & \cdots & 0 \\
\sin\theta_2\cos\theta_3 & r\cos\theta_2\cos\theta_3 & \cdots & 0 \\
\vdots & \vdots & \ddots & \vdots \\
\sin\theta_2\ldots\sin\theta_{K-2}\cos\theta_{K-1} & r\cos\theta_2\ldots\sin\theta_{K-2}\cos\theta_{K-1} & \cdots & -r\sin\theta_2\ldots\sin\theta_{K-2}\sin\theta_{K-1} \\
\sin\theta_2\ldots\sin\theta_{K-2}\sin\theta_{K-1} & r\cos\theta_2\ldots\sin\theta_{K-2}\sin\theta_{K-1} & \cdots & r\sin\theta_2\ldots\sin\theta_{K-2}\cos\theta_{K-1}
\end{vmatrix}$$

$$= \left(r\cos^2\theta_1\left(\sin\theta_1\right)^{K-2} + r\sin^2\theta_1\left(\sin\theta_1\right)^{K-2}\right) J_{K-1}\left(r,\theta_2,\ldots,\theta_{K-1}\right)$$

$$= r\left(\sin\theta_1\right)^{K-2}\left[r^{K-2}\left(\sin\theta_2\right)^{K-3}\left(\sin\theta_3\right)^{K-4}\ldots\sin\theta_{K-2}\right]$$

$$= r^{K-1}\left(\sin\theta_1\right)^{K-2}\left(\sin\theta_2\right)^{K-3}\ldots\sin\theta_{K-2}$$

by the induction hypothesis, which is the desired formula for $n = K$.

# Appendix B.

**Summary of Probability Density Functions**

The following list provides, for ready reference, the probability density functions required in the body of the report. The variables, $x$; $x_1, x_2, \ldots, x_n$; $y_1, y_2, \ldots y_n$ are independent Gaussian random variables, each with zero mean and variance $\sigma^2$

$$p(x) = \frac{1}{\sigma\sqrt{2\pi}} e^{-x^2/2\sigma^2} \quad -\infty < x < \infty$$

$$p(w = x^2) = \frac{1}{\sigma\sqrt{2\pi}} w^{-1/2} e^{-w/2\sigma^2} \quad 0 < w < \infty$$

$$p\left(r = \sqrt{x_1^2 + x_2^2 + \ldots + x_n^2}\right) = \frac{2\left(\frac{1}{2}\right)^{n/2}}{\sigma^n \Gamma\left(\frac{n}{2}\right)} r^{n-1} e^{-r^2/2\sigma^2} \quad 0 \le r < \infty$$

$$p\left(u = x_1^2 + x_2^2 + \ldots + x_n^2\right) = \frac{\left(\frac{1}{2}\right)^{n/2}}{\sigma^n \Gamma\left(\frac{n}{2}\right)} u^{n/2-1} e^{-u/2\sigma^2} \quad 0 \le u < \infty$$

$$p\left(r = \sqrt{(x_1 - y_1)^2 + (x_2 - y_2)^2 + \ldots + (x_n - y_n)^2}\right) = \frac{2\left(\frac{1}{4}\right)^{n/2}}{\sigma^n \Gamma\left(\frac{n}{2}\right)} r^{n-1} e^{-r^2/4\sigma^2} \quad 0 \le r < \infty$$

$$p\left(u = (x_1 - y_1)^2 + (x_2 - y_2)^2 + \ldots + (x_n - y_n)^2\right) = \frac{\left(\frac{1}{4}\right)^{n/2}}{\sigma^n \Gamma\left(\frac{n}{2}\right)} u^{n/2-1} e^{-u/4\sigma^2} \quad 0 \le u < \infty$$

# Appendix C.

**Construction of a data set having "Ideal" Gaussian properties**

As mentioned in the text, computer-generated histograms of Gaussian distributions often (approximately 5% of the time) fail a chi-square Goodness-of-Fit test for normality. Such distributions are unacceptable representations of the background noise for the purposes of this analysis. Two such examples are shown in Fig. AB1 below.
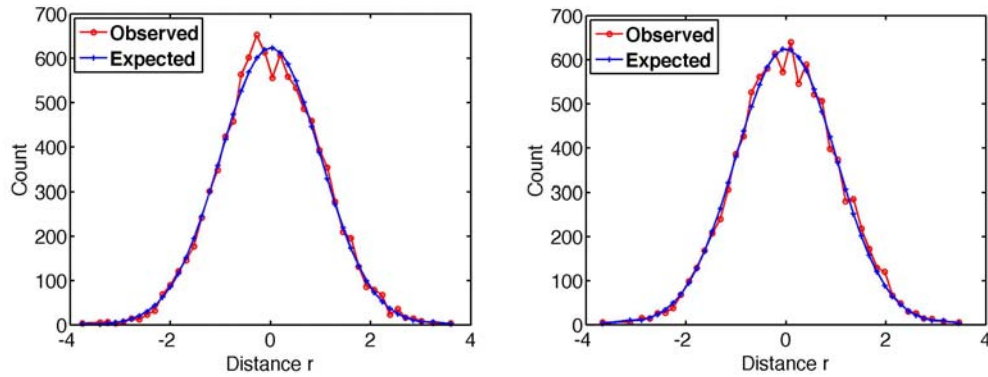


*Fig. C1* Two example plots showing the observed and expected counts associated with 10000 Gaussian deviates generated via the MATLAB random number generator. The number of bins was set to *K=50*. In both examples the data failed the chi-square Goodness-of-Fit test for threshold value $\chi_0^2 = 59.3$ (corresponding to a Type-I error of 5%).

To test the detection strategies in this paper a nearly perfect Gaussian representation of the noise is needed. In this Appendix, a method is shown to mathematically construct an ideal approximation to a Gaussian distribution of white noise; that is, a finite sequence of numbers with the following properties:

1) Gaussian-shaped histogram of amplitudes
2) Delta-function autocorrelation function and therefore a flat power spectral density function.

Consider the particular normal distribution *N*(0,1) with zero mean and unit variance. The probability that such a random variable x occurs in the range $a \leq x \leq b$ is given by

$$P\left(a \leq x \leq b\right) = \frac{1}{\sqrt{2\pi}} \int_a^b \exp(-x^2/2)dx = \frac{1}{2}\left[ erf\left(b/\sqrt{2}\right) - erf\left(a/\sqrt{2}\right)\right]$$

If x(t) is a time series whose values are independently sampled from the above distribution, then its autocorrelation function is given by[13]

$$R_{xx}(t, t+\tau) = E[x(t)x(t+\tau)] \xrightarrow[x \in N(0,1)]{} \delta(\tau)$$

and its two-sided power spectral density

$$S_{xx}(\omega) = \frac{1}{2\pi} \int_{-\infty}^{\infty} R_{xx}(\tau) e^{-j\omega\tau} d\tau \xrightarrow[x \in N(0,1)]{} \frac{1}{2\pi}$$

That is, the power spectral density is flat, independent of frequency.

The process for constructing a data vector having the desired properties is as follows.

1. Choose the number of points $M$ in the data vector, the number of bins $K$, and the maximum and minimum values of the histogram, xmax and xmin, respectively.

2. Then the width of each bin is $\Delta = (x \max - x \min)/K$,
bin edges occur at $x_e(k) = x \min + (k-1)\Delta$ for $k = 1, 2, \cdots, (K+1)$ (note that this includes the lower edge of the lowest bin and the upper edge of the upper bin), and bin centers occur at $x_c(j) = x \min + (j-1)\Delta/2$ for $j = 1, 2, \cdots, K$.
Hence there are $K$ bin centers but $(K+1)$ bin edges.

3. The exact (non-integer) number of entries in each bin is given by

$$v(j) = (M/2) \left| erf\left(x_e(j+1)/\sqrt{2}\right) - erf\left(x_e(j)/\sqrt{2}\right) \right|, \quad j = 1, 2, \cdots, K$$

.

We calculate the integer number of entries in each bin $v_r(j)$ using Matlab by rounding to the nearest integer, $v_r(j) = round(v(j))$. Hence, the "error" in the count in each bin is $dv(j) = v(j) - v_r(j)$.

4. Once the integer number of points in each bin, $v_r(j)$, is known we construct an actual set $S_j$ of data values for each bin by choosing the appropriate number of points from a uniform distribution on the interval of values using the rule:

$$S_j = \left\{ x_e(j) + \Delta\left(rand(v_r(j), 1)\right) \right\}.$$

Here, the Matlab function $rand(v_r(j), 1)$ returns a set of $v_r(j)$ values uniformly distributed on the interval $(0,1)$.

5. Append together all $K$ number sets $S_j$ to form an M-dimensional data vector $\vec{x}'$.
This data vector has the required property of Gaussian distribution of amplitudes but, due to the way the numbers were obtained, the ordering of the values contains

unwanted structure – structure that can be eliminated by properly "shuffling" the vector components. This is accomplished in Matlab by first generating a uniformly-distributed random vector $\vec{r}$ of the same length as $\vec{x}'$. The elements of $\vec{r}$ are then sorted in ascending (or descending) order. Since the elements of $\vec{r}$ are randomly distributed, the indices of the sorted values should be randomly distributed and we use this property to shuffle the ordering of the values in $\vec{x}'$. The values in $\vec{x}'$ are re-arranged using the indexing obtained from sorting the values in $\vec{r}$, resulting in the final data vector $\vec{x}$.

This final data vector now has all the required properties: 1) Gaussian distribution of amplitudes, 2) flat power spectral density, and 3) delta-function-like autocorrelation function.

It should be noted that the approach described above generally yields a histogram that is nearly, but not perfectly, Gaussian and that generally contains nearly, but not exactly, the number of points *M* specified at the beginning of the process. In some cases, the agreement can indeed be perfect but this is only an accident. The reason is simple. Although the fraction of the total number of points that should reside in any bin of the histogram can be calculated to any degree of precision, there is no guarantee that this fraction of the total number of points is an integer. Hence, the best we can do is to round the required number of points to the nearest integer. The resulting errors are surprisingly small as shown below.

Figure C.2 shows the histogram of actual (non-integer) values, the histogram of integer values, and the error in each of 32 bins for *M*=1024 data points. In this case the actual size of the data vector was 1026 .



(a)    (b)
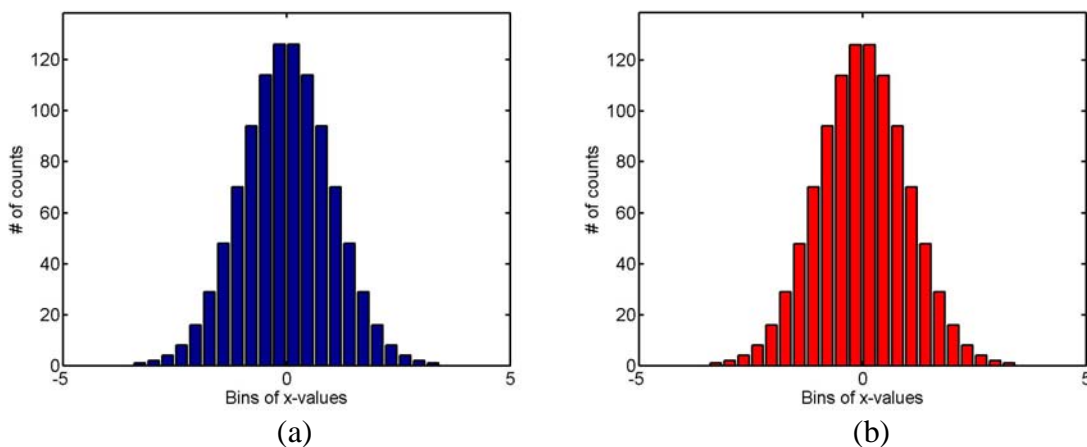
***Fig. C2.*** Comparison of histograms for (a) calculated (non-integer) values, and (b) values rounded to nearest integer.

These two histograms are nearly identical with differences in the counts in each bin due entirely to the rounding process. The differences, plotted below in Fig. C3, are no longer than approximately 0.5 counts.
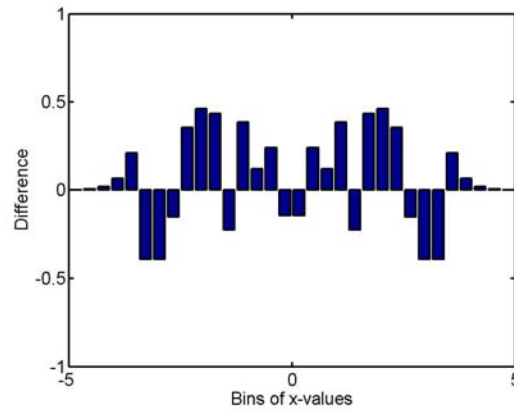


**Fig. C3.** Discrepancy in bin occupancy between actual values and rounded integer values.

The sets of values for each bin are shown in Fig. C4(a) while the shuffled version of the same set of values is shown in Fig.C4(b) indicating at least qualitatively the effectiveness of the shuffling procedure.



(a)                                              (b)
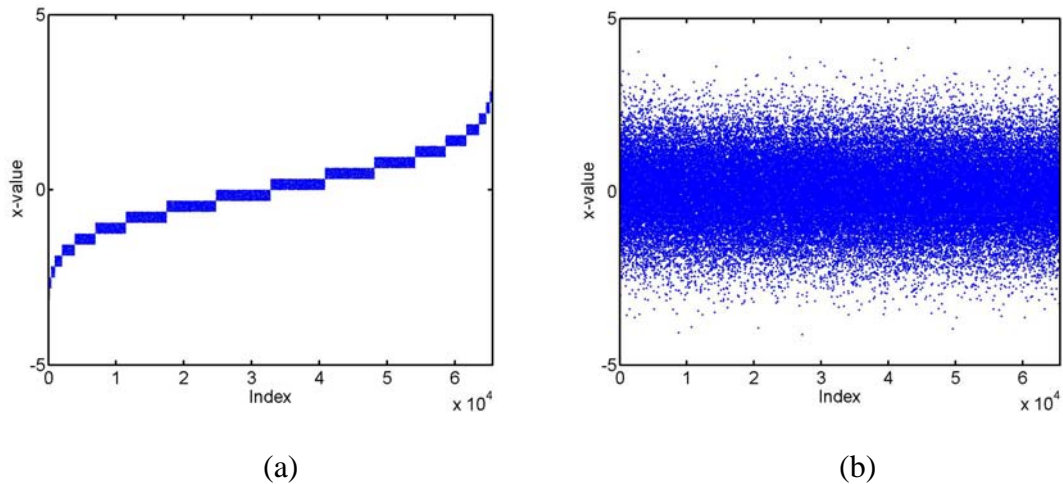
**Fig. C4.** Comparison of (a) ordered and (b) shuffled values.

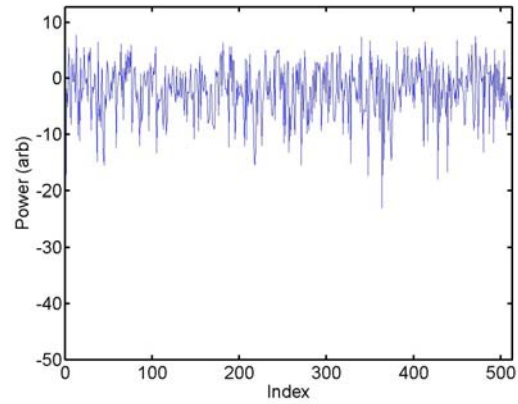Finally, the power spectrum and autocorrelation are shown in Figs. C5 and C6, respectively.



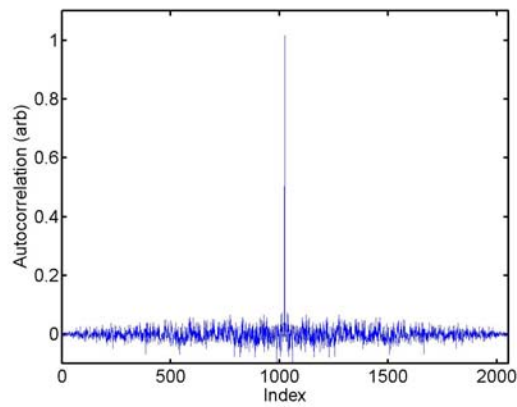Fig. C5. Power spectrum of the shuffled data vector in Fig. C4(b).



Fig. C6. Autocorrelation of the shuffled data vector in Fig. C4(b).

# References

[1] R. N. McDonough and A. D. Whalen, "Detection of Signals in Noise, 2nd edition", Academic Press, San Diego, Ca. 1995.

[2] J.-P Eckmann, S. O. Kamphorst, and D. Ruelle, "Recurrence Plots of Dynamical Systems", *Europhysics Letters*, **4**(9), pp. 973-977, 1987.

[3] N. Marwan, M. C. Romano, M. Thiel, and J. Kurths, "Recurrence Plots for the Analysis of Complex Systems", *Physics Reports*, **438**, pp. 237-329, 2007.

[4] J. P. Zbilut, A. Giuliani, and C. L. Webber Jr. "Recurrence Quantification Analysis and Principal Components in the Detection of Short Complex Signals", *Physics Letters A*, **237**, pp. 131-135, 1998.

[5] J. P. Zbilut, A. Giuliani, and C. L. Webber Jr. "Detecting Deterministic Signals in Exceptionally Noisy Environments Using Cross-Recurrence Quantification", *Physics Letters A*, **246**, pp. 122-128, 1998.

[6] J. P. Zbilut, A. Giuliani, and C. L. Webber Jr. "Recurrence Quantification Analysis as an Empirical Test to Distinguish Relatively Short Deterministic Versus Random Number Series", *Physics Letters A*, **267**, pp. 174-178, 2000.

[7] G. Filligoi and F. Felici, "Detection of Hidden Rhythms in Surface EMG signals with a Non-Linear Time-Series Tool", *Medical Engineering & Physics*, **21**, pp. 439-448, 1999.

[8] B. M. Dissinger, G. K. Rhode, R. B. Rhodes, Jr., F. Bucholtz, and J. M. Nichols, "Intensity Analysis of Recurrence Plots for the Detection of Deterministic Signals in Noise", Naval Research Laboratory Report NRL/MR/5650—06-9004, Dec. 12, 2006.

[9] G. K. Rhode, J. M. Nichols, F. Bucholtz, and B. M. Dissinger, "Stochastic Analysis of Recurrence Plots with Applications to the Detection of Deterministic Signals". (submitted for publication to *Physica D*).

[10] L. M. Pecora, L. Moniz, J. M. Nichols, and T. Carroll, "A Unified Approach to Attractor Reconstruction". *Chaos* **17**, 013110, 2007.

[11] E. Parzen, "Modern Probability Theory and its Applications", John Wiley & Sons, Inc., New York, 1960.

[12] T. Schreiber and A. Schmitz, "Discrimination Power of Measures for Nonlinearity in a Time Series", Physical Review E., **55**(5), pp. 5443-5447, 1997.

[13] J. S. Bendat and A. G. Pierson, "Random Data Analysis and Measurement Procedures, 3rd Edition", John Wiley & Sons, Inc., New York, 2000.